Int. J. Heat Mass Transfer. Vol. 32, No. 4, pp. 711–722, 1989
Printed in Great Britain

0017–9310/89 $3.00 + 0.00

Heat transfer characteristics of the annulus of two-coaxial cylinders with one cylinder rotating

YONG N. LEE
Heat Transfer Research & Development, Ltd., 1010 W. Lonnquist Blvd.,
Mt. Prospect, IL 60056, U.S.A.

and

W. J. MINKOWYCZ
Department of Mechanical Engineering, University of Illinois,
Box 4348, Chicago, IL 60680, U.S.A.

(*Received* 10 *May* 1988 *and in final form* 15 *August* 1988)

Abstract—The heat transfer characteristics of two coaxial cylinders, one of which is rotating, are investigated experimentally in the range of Taylor numbers $(Ta)_m$ from 10^3 to 2×10^7 with the axial Reynolds numbers Re from 50 to 1000. Mass transfer measurements of naphthalene are made to obtain the heat transfer coefficients. Four configurations of the coaxial systems are chosen to investigate fundamental phenomena occurring in the annuli of various combinations of the coaxial systems. The surfaces of the cylinders constituting the annuli are either smooth or one smooth and the other grooved axially. Preliminary pressure drop measurements are made on some configurations. The results obtained through the present research suggest that there is a potential merit for further investigation in applications where high density heat transfer is required.

1. INTRODUCTION

COMPONENTS of many mechanical systems such as wet clutches of vehicles, mechanical seals, or electric motors have one thing in common: one of the elements constituting each component rotates either as a disc or cylinder. In these components, an effective removal of heat is important due to the growing demand for high compactness.

The objective of the present investigation is to explore the condition under which the components can operate with high heat dissipation to fluid flowing between the stationary and rotating elements.

To this end, the heat transfer characteristics of the annuli of four configurations of two coaxial cylinders with one of them rotating have been studied. For potential applications to compact heat exchangers, preliminary studies of the pressure drop characteristics have also been made. The cylinder surfaces which constitute the annulus are smooth or grooved. The grooves are made in the longitudinal direction of the cylinder.

Since the pioneering work by Taylor [1] on the stability of non-flowing fluid in the annulus of a coaxial cylindrical system with the inner cylinder rotating, the heat transfer problem of this configuration with positive axial flow has been investigated by several investigators [2–5]. Their work mainly concerned the characteristics on long cylinders $(L/D_h > 36)$ where the velocity and temperature distributions are in a fully developed condition. However, configurations in most of the practical cases have both the fluid velocity and temperature still developing. Only limited data are available on rotating internal cylinders through works done by prior investigators [6, 7]. No data are available to the authors' knowledge on rotating external cylinders. The results of the fully developed flow cylinder systems studied by the previous investigators on rotating internal cylinders, nevertheless, showed that heat transfer is greatly enhanced as the rotational speed increases beyond a critical value, which is similar to Taylor's critical rotational speed. The present study is motivated from this preliminary work conducted by the prior investigators.

The present work investigates experimentally the heat transfer enhancement characteristics in the annuli of two coaxial short cylinders $(L/D_h < 12.5)$ with one cylinder rotating, as well as its pressure drop characteristics. From the argument made in the preceding paragraph, it is implied that the present work corresponds to entrance region heat transfer studies in the annulus of two coaxial cylinders, one of which is rotating.

The fact that the entrance regime will depend on more experimental variables than the fully developed regime suggests that the experimental setup should be flexible, particularly capable of handling varying lengths of heat transfer surface. To build an experimental setup allowing such flexibilities with conventional heat transfer measurements is extremely costly. In addition to the cost, conventional heat

NOMENCLATURE

b	minimum annulus gap [mm]
b_m	annulus gap of grooved cylinder, equation (5) [mm]
D_h	hydraulic diameter [mm]
e	surface roughness [mm]
f	coefficient of friction [mm]
F_g	geometric factor, equation (8) [mm]
GD	groove depth [mm]
GW	groove width [mm]
h	heat transfer coefficient of smooth cylinders [$W cm^{-2} K^{-1}$]
$(ha)_m$	heat transfer coefficient based on total surface area including grooves [$W cm^{-2} K^{-1}$]
k	thermal conductivity of fluid [$W cm^{-1} K^{-1}$]
L	cylinder length [mm]
Nu_{D_h}	Nusselt number based on equation (3) [—]
Nu_m	Nusselt number based on total area [—]
Nu_j	Nusselt number based on projected area [—]
ΔP	pressure drop [$N m^{-2}$]
Pr	Prandtl number [—]
R	cylinder radius [mm]
Re_e	effective Reynolds number, equation (2) [—]
Re	Reynolds number based on D_h [—]
RGL	arc length of a groove [—]
RL	length of cylinder [mm]
$RLID$	groove base i.d. of rotating outer cylinder [mm]
$RLOD$	o.d. of grooved rotating cylinder [mm]
R_m	average radius of cylinders [mm]
ROD	o.d. of rotating cylinder [mm]
RSL	arc length of groove pitch on o.d. [mm]
$RSOD$	groove base o.d. of rotating cylinder [mm]
$RSID$	i.d. of grooved rotating outer cylinder [mm]
S	geometric parameter, equation (9) [—]
SID	i.d. of stationary cylinder [mm]
$SLID$	groove base i.d. of stationary cylinder [mm]
$SSID$	i.d. of grooved stationary cylinder [mm]
SOD	o.d. of stationary cylinder [mm]
$(Ta)_m$	Taylor number based upon b_m, equation (7) [—]
Ta	Taylor number based on b [—]
U_r	peripheral velocity [$m s^{-1}$]
V_a	axial flow velocity in smooth annulus [$m s^{-1}$]
V_e	effective velocity, equation (1) [$m s^{-1}$]
V_{max}	axial flow velocity through grooved annulus [$m s^{-1}$].

Greek symbols

μ	dynamic viscosity [$N s m^{-2}$]
ν	kinematic viscosity [$m^2 s^{-1}$]
ρ	density of fluid [$g cm^{-3}$]
ω	angular velocity [$rad s^{-1}$].

transfer measurements have increasing uncertainties either due to heat leakage with high temperature difference (high heat flux density) or due to temperature measurement uncertainties at low heat flux densities. For this reason, heat transfer data are obtained in the present work using the naphthalene sublimation technique which utilizes the analogy between convective mass and heat transfer processes. As shown later in the main body of this paper, however, the entrance effect is negligible on grooved cylinders.

A detailed discussion on the basis of the technique is found in refs. [8, 9]. In brief, the amount of naphthalene mass sublimed into the air stream from a solid naphthalene surface the contour of which is similar to the heat transfer surface under study, is equivalent to the amount of heat transferred from the heat transfer surface to the fluid stream flowing over it. The experimental simplicity can be readily conceived, since any solid surface which is coated with naphthalene constitutes a similar heat transfer surface at a constant temperature dissipating heat, while an uncoated surface constitutes an insulated surface. The validity of the naphthalene sublimation technique is demonstrated in Section 3 via reproducing heat transfer data published in the open literature.

The experimental setup incorporated with the naphthalene tests is described in detail in Section 2. In brief, the test section consists of cylinders made of aluminum and the surface under investigation is coated with naphthalene to a thickness of 0.125 mm to a desired length (63.5–127 mm). The minimum internal diameters of the outer cylinder ranged from 106.7 to 133.3 mm; the maximum outside diameters of the inner cylinder ranged from 104.9 to 131.7 mm. A more detailed description of the test section will be presented later.

Only one of the cylinders is coated with naphthalene for a set of experiments to single out the heat transfer coefficient of the particular cylinder. The rotational speed ranged from 50 to 4000 r.p.m.; the Taylor numbers $(Ta)_m$ ranged from 10^3 to 2×10^7. The axial airflow rates were set to cover axial flow Reynolds numbers Re from 52 to 1000.

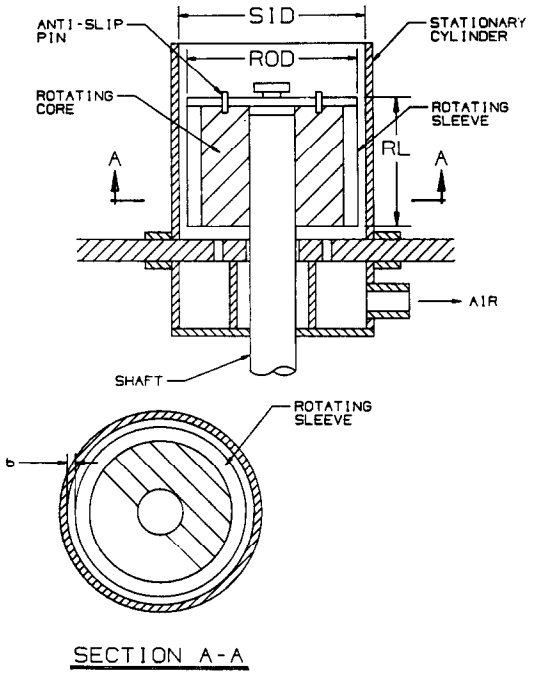

FIG. 1. Construction of Configuration (A). Mass transfer surface: inner smooth rotating.

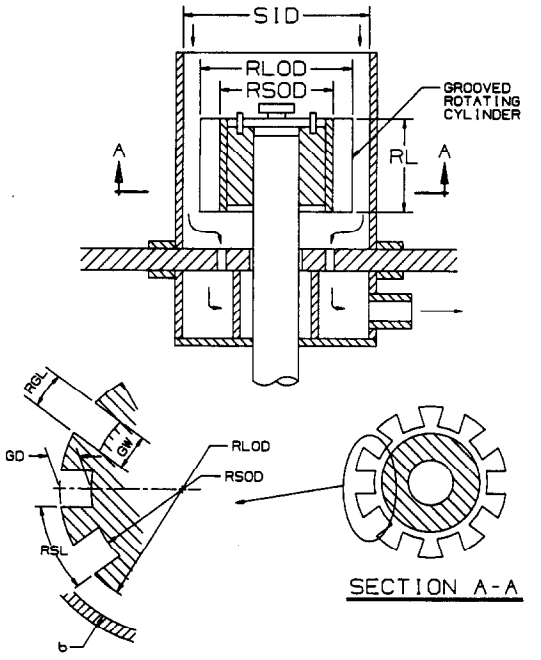

FIG. 2. Construction of Configuration (B). Mass transfer surface: inner grooved rotating.

2. EXPERIMENTAL APPARATUS AND PROCEDURES

2.1. *Test section configurations and assembly*

A total of four configurations have been used in the present study: Configurations (A)–(D). Figure 1 shows a cross-sectional view of the test section for Configuration (A). The smooth cylindrical core (sleeve holder) made of Lexan rotates with the shaft. A cylindrical sleeve made of Lexan, the external and internal surfaces of which are smooth, is fit on to the core so that the sleeve rotates with the core. The external surface of the sleeve is the heat (mass) transfer surface. A provision is made against a possible slip between the core and the sleeve by installing two anti-slip pins. With installation of the aluminum stationary outer smooth cylinder, the test section for testing Configuration (A) is formed. Figure 2 shows the structure of the test section for studying Configuration (B).

The test section is identical to that of Configuration (A) except that the rotating cylindrical sleeve is made with aluminum and has a grooved external surface.

Figure 3 shows the test section for studying Configuration (C) in which the outer stationary cylinder is under investigation and has grooves. As with Configurations (A) and (B), a sleeve is inserted into the stationary outer cylinder.

The heat (mass) transfer surface is the internal surface of the sleeve. Figure 4 shows the test section for studying Configuration (D) in which the outer grooved cylinder under investigation rotates.

As illustrated above, the cylinder under investigation consists of two components: the sleeve with the surface under investigation and the holder holding the sleeve.

After each test run, the sleeve is removed from the holder to measure the weight of the sleeve to determine the weight loss of naphthalene during the run as described later. There are two basic types of sleeves used in the present study. A sleeve composed of two half sleeves is used to investigate the characteristics of the grooved outer cylinder. Splitting of the sleeve into two halves is needed for coating of naphthalene over the internal surface of the outer cylinder. Either a

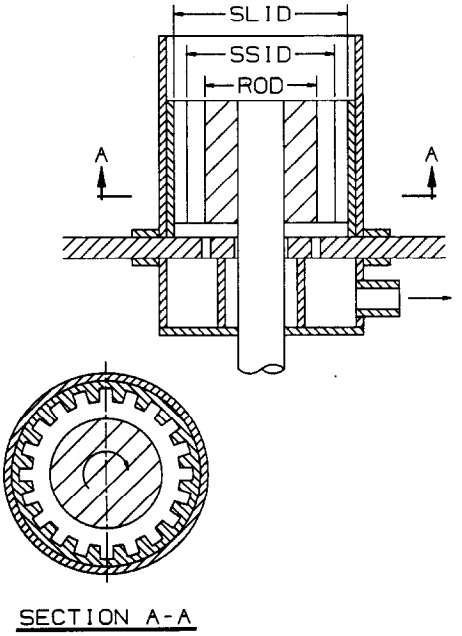

FIG. 3. Construction of Configuration (C). Mass transfer surface: outer grooved stationary.

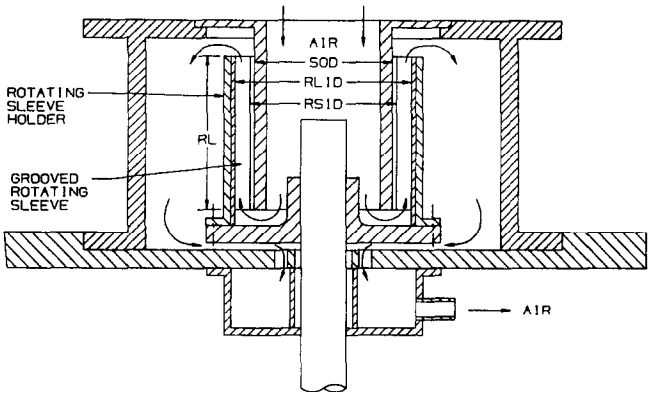

FIG. 4. Construction of Configuration (D). Mass transfer surface: outer grooved rotating.

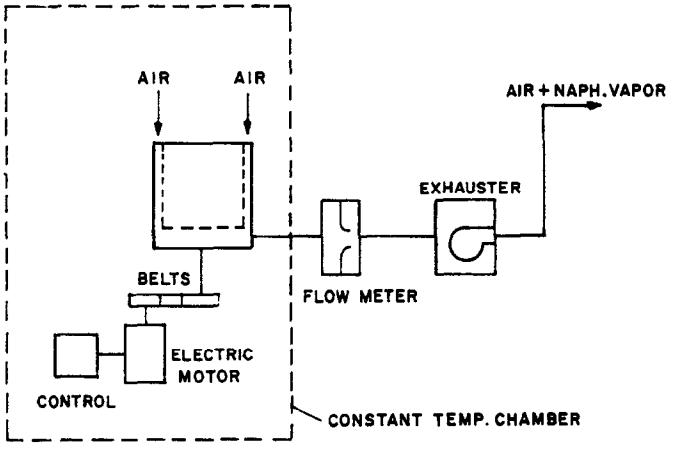

FIG. 5. Experimental rig.

knob or two screws are used for fitting the sleeve onto the holder or for lifting to remove the sleeve from the holder.

The test sections described above are a part of the total test section assembly to be installed inside the supply air chamber which is maintained at a constant temperature (Fig. 5).

2.2. *Geometries of test sections*

Table 1 shows the principal dimensions of the test sections used. Definitions of the variables are shown in Figs. 1–4.

2.3. *Test rig and procedures*

The main features of the test rig are given in detail in refs. [8, 9]. In brief, a number of mass transfer models prepared as per the procedures described above are stored in a constant temperature chamber kept at $25 \pm 0.1°C$ until they reach equilibrium temperature. The experimental rig is contained in this chamber as shown in Fig. 5. The chamber itself is housed in a larger, well insulated room. The room temperature is also controlled to maintain a temperature of $25 \pm 1°C$.

The primary quantity required for the evaluation

Table 1

Configurations	Mass transfer cylinder				
		SID	*ROD*		
(A)	Inner rotating (smooth)	127.0	111.1		
		SID	*RLOD*	*RSOD*	*GW*
(B)	Inner rotating (grooved)	133.4	131.7	111.0	10.34
			126.6	111.0	10.34
			121.5	111.0	10.34
		SLID	*SSID*	*ROD*	*GW*
(C)	Outer stationary (grooved)	127.0	106.7	104.9	10.16
		SOD	*RLID*	*RSID*	*GW*
(D)	Outer rotating (grooved)	104.9	127.0	106.7	10.16
				109.2	10.16

All dimensions are in mm.

of the mass transfer coefficient is the loss of mass during a data run. This quantity is obtained from weighing the mass transfer model (sleeve) immediately before and after the run. The mass transfer measurements are made with a precision balance (Mettler H315). The resolution of the balance is 10^{-4} g. The measured loss of mass is controlled at approximately 0.150 g or higher. Another quantity needed in the data reduction is the naphthalene vapor density at the mass transfer surface, which is determined from a vapor pressure–temperature relation [10].

The run times are adjusted so that the mass loss is sufficient for the required accuracy of data; however, the change in the thickness of the naphthalene coating during a data run is negligibly small.

Pressure drop measurements are made with the test sections without a naphthalene coating via a manometer with a resolution of 0.254 mm WG. The pressure drop data through the annulus with no rotational motion are baseline data and they are determined first before making major pressure drop measurements. To obtain data, the following procedures are taken. First, the test section sleeve, either for the inner or outer cylinder, is removed from the holder to allow air to flow through the test section with negligible flow resistance. Then, pressure drop measurements are made at different flow rates between the atmosphere and the downstream location of the test section. The results are used for correcting data in all pressure drop measurements.

2.4. *Preparation of mass transfer models*

A spray technique is used in the preparation of the mass transfer models. A sketch of the spray technique apparatus is shown in Fig. 6. Compressed air supplied from a high pressure air source '1' is used as primary air for atomizing liquid naphthalene. The primary airflow is regulated with primary control valve '2' which controls airflow and pressure depression at air nozzle '4'. The primary air is heated at primary heater '3'. Molten naphthalene in the reservoir '5' is discharged through liquid nozzle '6'. The secondary air after being heated at air heater '7' raises the air temperature of the enclosure which contains the spray system. Thus, hot air is entrained as the primary jet activates. A separate mechanical system is placed under the jet stream, which is capable of traversing a platform powered by an electrical motor. A cylindrical core, which is similar to the rotating core as discussed earlier, rotates via another motor mounted on the platform. The sleeves for studies of Configurations (A) and (B) are fitted onto the core. The two motors are used to control the traversing motion of the platform and rotating motion of the sleeve independently. With the simultaneous action of traversing and rotating motions, the sleeve receives liquid naphthalene uniformly. For coating internal surfaces of the outer cylinder sleeve, the mechanical system described above is not practical, and the coating is performed manually. The enhanced capability of coating the internal surface of the outer cylinder will be the subject of our future research. All other surfaces except the surface under investigation is covered with tape before the coating. The thickness of the coated layer is controlled at 0.125 mm. A check of the overall thickness of the plates showed that the thickness is uniform within 5%. The surface roughness condition can also be controlled with the control of external conditions such as position of the liquid nozzle with respect to the primary jet nozzle, primary jet velocity, temperature of air being entrained and that of the metal substrate, etc. Under appropriate conditions, the roughness height of the surface e can be held within 0.035 mm.

3. VALIDITY OF NAPHTHALENE SUBLIMATION TECHNIQUE

In order to examine the validity of the technique, a case of known results published are re-examined by the present technique. Gazley [2] obtained data using a long ($L/D_h = 36$) rotating cylinder in a concentric stationary cylinder. He defined an effective velocity to ascertain what combination of axial and rotational velocities determines the convective heat transfer rate; he used this velocity for evaluating the Reynolds number in establishing a general design correlation. The definition of his 'effective velocity' V_e is

$$V_e = [V_a^2 + (U_r/2)^2]^{0.5} \tag{1}$$

where V_a is the axial flow velocity; U_r the peripheral velocity of a rotating cylinder surface. The effective Reynolds number is defined by

$$Re_e = \rho V_e D_h/\mu. \tag{2}$$

The Nusselt number is defined by

$$Nu_{D_h} = hD_h/k \tag{3}$$

where D_h is the conventional definition of hydraulic diameter. Gazley's gap-to-mean radius is $b/R_m = 0.1$.

The present test results with the ratio of $b/R_m = 0.0804$ are shown in Fig. 7. As shown, Gazley's results are very close to those of the present work.

4. PERTINENT EXPERIMENTAL PARAMETERS

4.1. *Heat transfer*

Reviewing the works conducted by Gazley [2], Becker and Kaye [3], and Payne and Martin [6], the heat transfer data in the present work can be expressed in the functional form

$$Nu_m = \text{FUNCTION}((Ta)_m, Re, Pr) \tag{4}$$

with the length-to-hydraulic diameter ratio L/D_h or the gap ratio b/R as geometrical parameters, where R is the cylinder radius. In equation (4), Nu_m is the Nusselt number based on a characteristic length

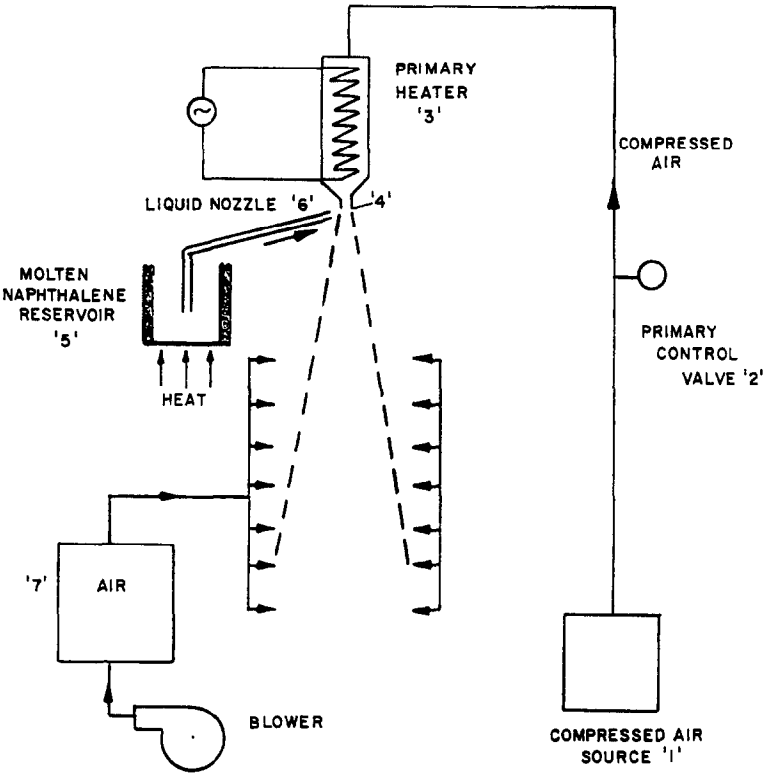

FIG. 6. Naphthalene spray system.

defined as twice the weighted average gap and the heat transfer coefficient $(ha)_m$ based on the total surface area including the groove area; thus, the Nusselt number Nu_m is defined by

$$Nu_m = (ha)_m(2b_m)/k \tag{5}$$

where the weighted average gap b_m is defined, referring to Fig. 2, by

$$b_m = b_{mm}/RSL \tag{6}$$

where

$$b_{mm} = b(RSL-RGL)+(GD+b)RGL$$

$(Ta)_m$ is the Taylor number defined by

$$(Ta)_m = (\omega^2 R_m b_m^3/\nu^2)(1/F_g) \tag{7}$$

where ω is the angular velocity of the rotating cylinder; R_m the average radius of the annulus based on b_m; and F_g a geometric factor defined by

$$F_g = (3.1417^4/41.2^2)[1-b_m/(2R_m)]^{-2}/S \tag{8}$$

$$S = 0.0571[1-0.652((b_m/R_m)/(1-b_m/(2R_m)))]$$
$$+0.00056/[1-0.652((b_m/R_m)/(1-b_m/(2R_m)))]. \tag{9}$$

Re is the Reynolds number for the axial flow based on the hydraulic diameter, D_h. Pr is the Prandtl number of the fluid.

In the limiting case of smooth cylinders, $b = b_m$; $Nu_m = Nu_j$, and $(Ta)_m = Ta$, where Nu_j is the Nusselt number based on the projected area for the grooved cylinders or on the surface area for smooth cylinders; Ta is the Taylor number based on the minimum gap b.

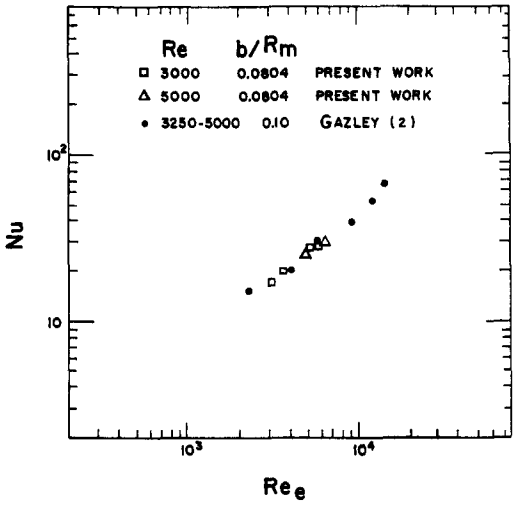

FIG. 7. Comparison with Gazley's heat transfer data.

4.2. *Pressure drop*

The pressure drop characteristics of the coaxial cylinders under investigation are expressed in terms of the coefficient of friction f and the axial Reynolds number Re with rotational speed as a parameter. The coefficient of friction is defined by

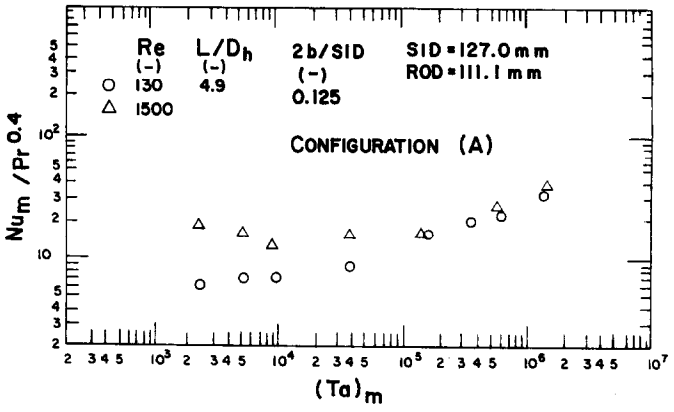

FIG. 8. Heat transfer results of Configuration (A).

$$\Delta P = (\text{dynamic head}) f(L/D_h) \quad (10)$$

where

$$\text{dynamic head} = 0.5\rho V_{max}^2 \quad (11)$$

and V_{max} is the mean velocity of fluid through the annulus.

5. EXPERIMENTAL RESULTS

5.1. *Heat transfer*

Heat transfer data for Configuration (A) of smooth cylinders are shown in Fig. 8 with $Re = 130$ and 1500. In order to make the results general, $Nu_m/Pr^{0.4}$ is used instead of Nu_m as the ordinate. It is seen that the Nusselt number Nu_m increases with Re at low Taylor numbers $(Ta)_m$ but that the effect of the Reynolds number diminishes at high values of $(Ta)_m$. It is also noted that there exists a $(Ta)_m$ for a given Re, beyond which the Nusselt number increases rapidly.

The trend of data above qualitatively agree with the results of previous investigators [3, 4]. The fact that the heat transfer results are insensitive to the Reynolds number at high $(Ta)_m$, seems to indicate that the entrance effect is negligible at high $(Ta)_m$, signaling that the Taylor vorticity effect has a predominant impact over other considerations such as developing flow.

The data of smooth cylinders presented above will serve as baseline data against the data of grooved cylinders to be presented in the following.

It was seen above for Configuration (A) that the entrance effect clearly exists at low $(Ta)_m$'s. To see if such a trend exists in Configuration (B) in which the inner cylinder has grooves, three sets of data are obtained with $RLOD = 131.7$, 126.6 and 121.5 mm with various coated lengths and Reynolds numbers. The results are shown in Figs. 9–11. As shown, the effects of length and Reynolds number are negligible, which suggests that the entrance length becomes very short with the existence of grooves. Comparison of the above three figures provides an interesting insight. The Nusselt numbers of Fig. 9 are lower than those of Figs. 10 and 11 which are close to each other. For this reason, the results of Figs. 10 and 11 are superimposed on Fig. 12, which suggests that, for $460 < Re < 1000$ and for the gap ratio $2b/SID > 0.051$, there is a possibility that a simple correlation may exist. The low Nusselt number of Fig. 9 may be attributed to the suppression of the Taylor vorticity at the minimum gap b.

To this effect, it is interesting to note that the value of the gap ratio equals 0.0127 for Fig. 9 is much smaller than 0.051 for Figs. 10 and 11, and that the Taylor number Ta based on the minimum gap b for Fig. 9 ranges from 10 to 10^4. With the lack of prior works, it may be reasonable to interpret the significance as per the result of Fig. 8, which suggests that critical Taylor numbers have not been reached in this range and the minimum gap area is not contributing toward the Taylor vorticity-controlled heat (mass) transfer.

Figure 13 shows the test results of Configuration (C) where the stationary outer cylinder has grooves and the rotating cylinder has a smooth surface (gap ratio of 0.0083). There appears to be a minor Reynolds number effect. But, it is remarkable to observe that the trend of data is similar to that of the inner rotating cylinder with a gap ratio of 0.0127.

Figure 14 shows the results of Configuration (D) where the grooved rotating outer cylinder (gap ratios of 0.0169 and 0.0394) constitutes the heat transfer surfaces. It is interesting to see the Nusselt numbers are similar to those of Configuration (B) with a gap ratio of 0.0127, since the Taylor vorticity does not influence the heat transfer in the minimum gap area in both cases with the enhancement of heat transfer mainly being due to vorticity within the grooves.

5.2. *Pressure drop*

Figures 15–17 show the pressure drop results of Configuration (B) with $RLOD = 131.7$, 126.6 and 121.5 mm, respectively, using the rotational speed as a parameter. The internal diameter of the smooth stationary cylinder SID is fixed constant at $SID = 133.4$ mm. It is seen that the rotational speed has a significant impact on the pressure drop charac-

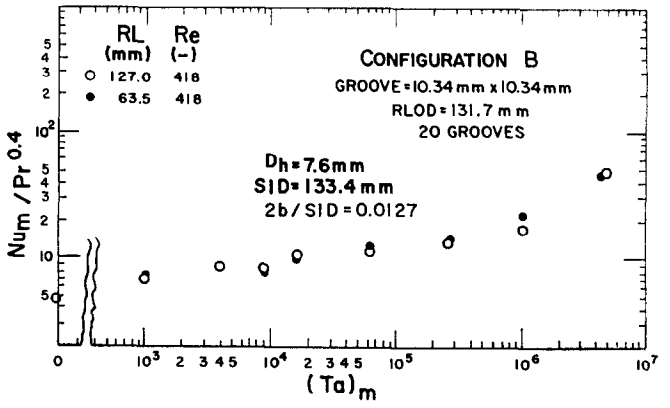

FIG. 9. Heat transfer results of Configuration (B). Groove: 10.3 × 10.3 mm.

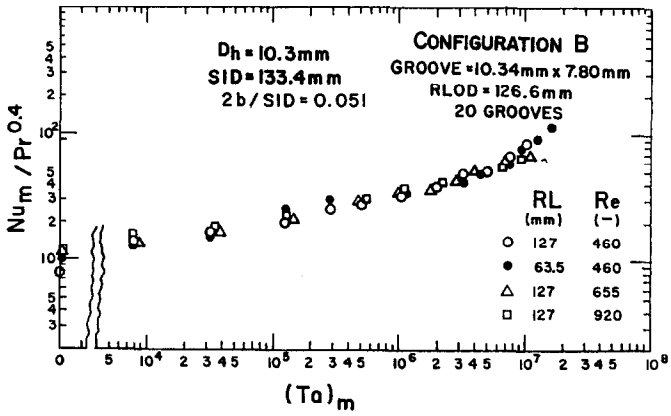

FIG. 10. Heat transfer results of Configuration (B). Groove: 10.3 × 7.8 mm.

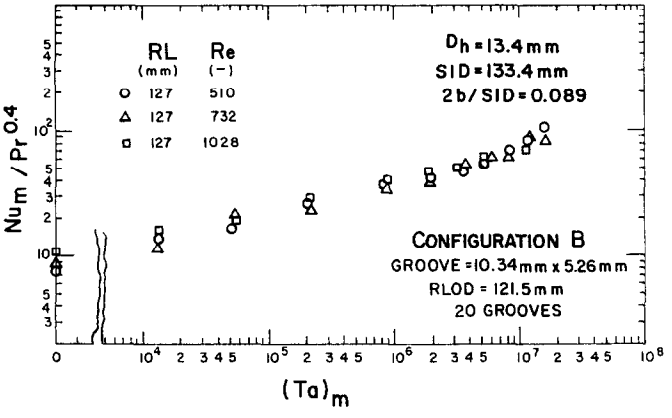

FIG. 11. Heat transfer results of Configuration (B). Groove: 10.3 × 5.3 mm.

teristics, and that, within the range of the present experimental work, the coefficient always increases with the rotational speed. However, at low rotational speeds, the effect is small. For $Re < 2000$, for instance, the effect is negligible up to 200 r.p.m.

The high coefficient of friction at high rotational speeds may be beneficial to the cases where high heat transfer is required with minimum consumption of coolant.

The pressure drop studies of Configuration (A) are not conducted in the present work, and those of Configurations (C) and (D) required more sophisticated instrumentation than the present scope of work calls for and left for future research opportunities.

6. RECENT WORKS BY OTHER INVESTIGATORS

Recent works by other investigators relevant to the present work are listed in refs. [4, 5, 11–18]. References [5, 17, 18] are excellent presentations of the development of Taylor vortices. References [13, 16] dealt with the effect of mixed convection. Mochizuki and

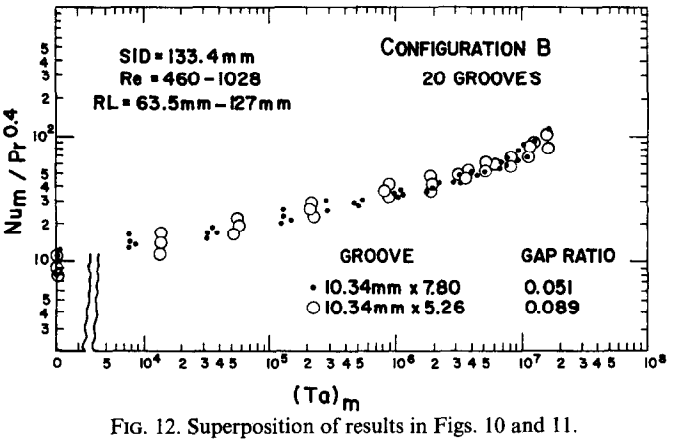

FIG. 12. Superposition of results in Figs. 10 and 11.

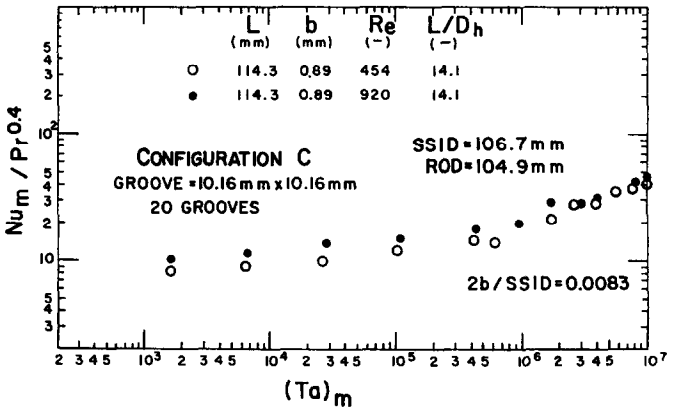

FIG. 13. Heat transfer results of Configuration (C). Groove: 10.3 × 10.3 mm.

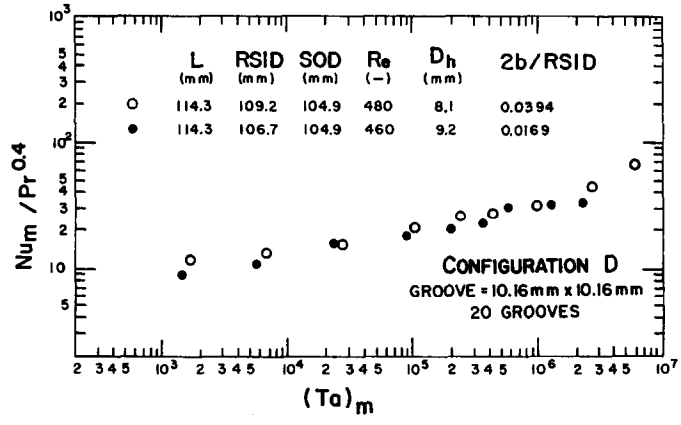

FIG. 14. Heat transfer results of Configuration (D). Groove: 10.3 × 10.3 mm.

Yang [12] studied the heat transfer and pressure drop characteristics of rotating annular disks.

Forced convection-dominant heat transfer of rotating rods and fins was investigated by Sparrow and Kadle [15] and that of the rotating cup-like cavity was studied by Sparrow and Chaboki [14]. They used the naphthalene sublimation technique which the present investigation also applied in the heat transfer studies. Gardiner and Sabersky [4] used a long annulus similar to that of the present work. However, their heat transfer data cannot be compared with the present results, since the heat transfer coefficients are based on the temperature difference between the rotating and stationary cylinder surfaces. Their pressure drop results with the inner slotted cylinder rotating are relevant to those of Configuration (B) of the present work. However, the groove geometries are so different that no direct comparison of data was attempted. Simmers and Coney [11] investigated the annulus similar to Configuration (C) of the present work. However, their stationary cylinder has a smooth surface rather than a grooved one, and no direct com-

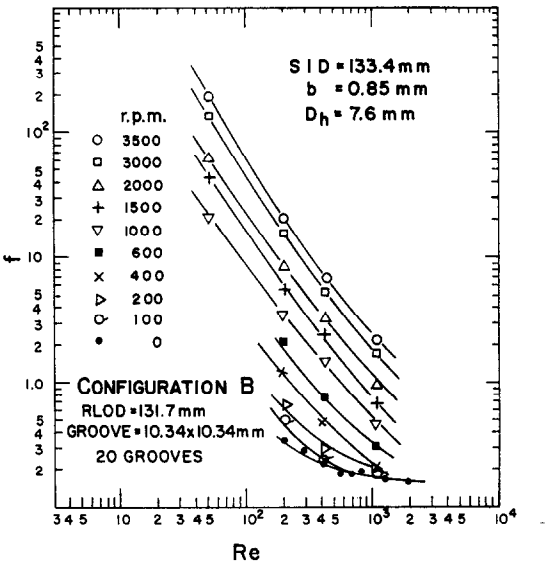

FIG. 15. Friction coefficient of Configuration (B). Groove: 10.3 × 10.3 mm.

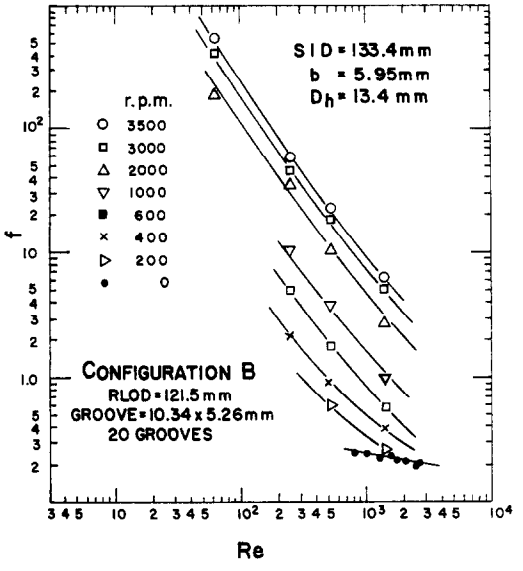

FIG. 17. Friction coefficient of Configuration (B). Groove: 10.3 × 5.3 mm.

parison is possible between the present data and theirs.

7. DISCUSSION OF RESULTS

The results presented in the preceding discussion in terms of parameters Nu_m and $(Ta)_m$, will serve as building blocks for establishing global correlations to be developed eventually; Nu_m is based on the total surface area including that of grooves and $(Ta)_m$ is based on the weighted average gap b_m.

However, to present the heat transfer results so as to provide a more practical significance, the Nusselt number Nu_j based on the projected area of the heat transfer surface and the Taylor number Ta based on the minimum gap b are more appropriate parameters. Figure 18 shows the summary of all heat transfer results plotted in terms of Nu_j and Ta where the Reynolds number effect is negligible. As discussed earlier, the Reynolds number effect on heat transfer is negligible except in Configuration (A). From this summary, the following conclusions can be made.

(1) The presence of grooves on the rotating inner cylinder significantly increases Nu_j over the smooth cylinder.

(2) For either Configuration (B) or Configuration (D), large gap ratios (>0.0394) are desirable for high heat transfer. This feature will be beneficial where low pressure drop through the annulus is desired for a given flow.

(3) The Nusselt numbers of all configurations having grooves appear to follow a simple correlation at high Ta's for the groove geometries of the present work: 10.3 × 10.3, 10.3 × 7.8 and 10.3 × 5.3 mm.

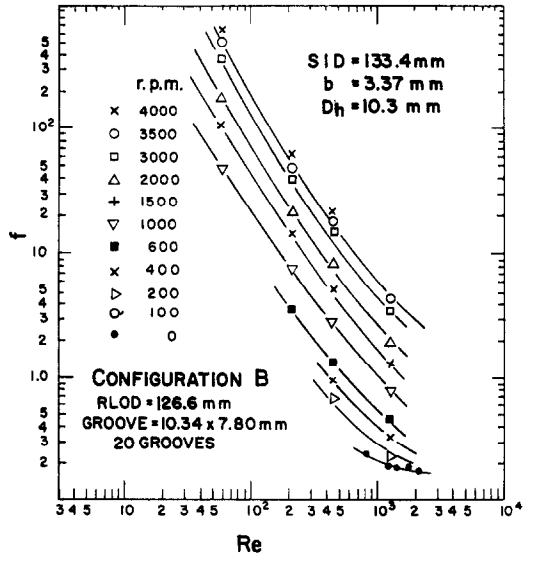

FIG. 16. Friction coefficient of Configuration (B). Groove: 10.3 × 7.8 mm.

To provide a further insight into a heat exchange device where high heat transfer but low pressure drop are required, consider Configuration (B) of Fig. 18. The Taylor number corresponding to 3000 r.p.m. is $Ta = 7.9 \times 10^5$. The Nusselt number at this Ta and $Re = 920$ is $Nu_j/Pr^{0.4} = 55$; the coefficient of friction $f = 5.0$ from Fig. 16. At 0 r.p.m., $Ta = 0$. The Nusselt number $Nu_j/Pr^{0.4}$ at $Ta = 0$ and $Re = 920$ is approximately equal to 7.0; the coefficient of friction $f = 0.23$. Hence, the Nusselt number ratio and the friction coefficient ratio at 3000 and 0 r.p.m. are equal to 7.86 and 21.8, respectively. The friction coefficient ratio in this case is actually the pressure drop ratio of the rotating to non-rotating cylinder systems for a given flow rate. Suppose that the Nusselt number is increased by a factor of 7.86 only through the increase of the Reynolds number. Then, the pressure drop ratio

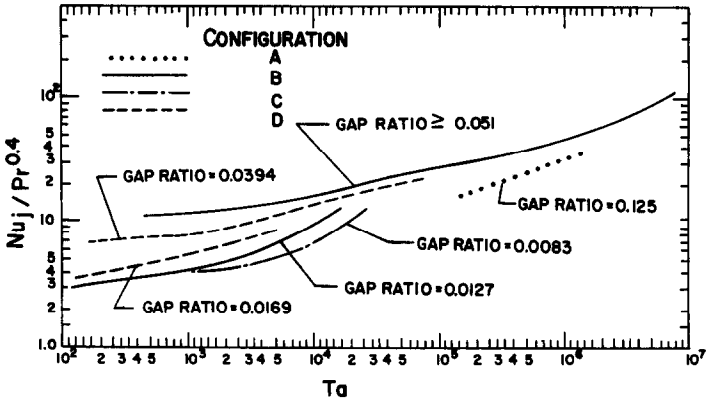

FIG. 18. Heat transfer results based on projected area: all configurations.

would increase by one order of magnitude higher than that of 21.8 obtained with the rotating system, which is undesirable under the present consideration.

8. CONCLUDING REMARKS

The results obtained through the present work concerning the heat transfer and pressure drop characteristics of the coaxial cylinder systems suggest that there are potential opportunities in the area of specialized heat exchange systems and provide incentives for further investigations.

Acknowledgement—The authors wish to acknowledge that this material is based upon work supported by the National Science Foundation under award number ISI-8660146.

REFERENCES

1. G. I. Taylor, Stability of viscous fluid between two rotating cylinders, *Phil. Trans. R. Soc. London*, Series A **223,** 289–343 (1923).
2. C. Gazley, Jr., Heat transfer characteristics of the rotation and axial flow between concentric cylinders, *ASME Trans.* **80,** 79–90 (1958).
3. K. M. Becker and J. Kaye, Measurements of diabatic flow in an annulus with an inner rotating cylinder, *J. Heat Transfer* 97–105 (1962).
4. S. R. M. Gardiner and R. H. Sabersky, Heat transfer in an annular gap, *Int. J. Heat Mass Transfer* **21,** 1458–1466 (1978).
5. H. L. Swinney and J. P. Gollub, *Topics in Applied Physics* (2nd Edn), Vol. 45. Springer, Berlin.
6. A. Payne and B. W. Martin, Heat transfer to laminar axial flow in a concentric annulus from a rotating inner cylinder, *Proc. Fifth Int. Heat Transfer Conf.* (1974).
7. K. N. Astill, Studies of the developing flow between concentric cylinders with the inner cylinder rotating, *J. Heat Transfer* 383–391 (1964).
8. Y. N. Lee, Heat transfer and pressure drop characteristics of an array of plates aligned at angles to the flow in a rectangular duct, *Int. J. Heat Mass Transfer* **29,** 1553–1563 (1986).
9. Y. N. Lee, Heat transfer and pressure drop characteristics of an assembly of partially segmented plates, presented at the ASME WAM, Anaheim, California (December 1986).
10. H. H. Sogin, Sublimation from disks to air streams flowing normal to their surfaces, *Trans. ASME* **80,** 61–71 (1958).
11. D. A. Simmers and J. E. R. Coney, A Reynolds analogy solution for the heat transfer and axial flows, *Int. J. Heat Mass Transfer* **22,** 679–698 (1979).
12. S. Mochizuki and W. Yang, Heat transfer and friction loss in laminar radial flows through rotating annular disks, *J. Heat Transfer* **103,** 212–217 (1981).
13. M. A. I. El-Shaarawi, Developing laminar free convection in an open ended vertical annulus with a rotating inner cylinder, *J. Heat Transfer* **103,** 552–558 (1981).
14. E. M. Sparrow and A. Chaboki, Heat transfer coefficients for a cup-like cavity rotating about its own axis, *Int. J. Heat Mass Transfer* **25,** 1333–1340 (1982).
15. E. M. Sparrow and D. S. Kadle, Heat transfer from rods or fins which extend radially outward from a rotating shaft, *J. Heat Transfer* **106,** 290–296 (1984).
16. T. Fusegi, B. Farouk and K. S. Ball, Mixed-convection flows within a horizontal concentric annulus with a heated rotating inner cylinder, *Numer. Heat Transfer* **9,** 591–614 (1986).
17. K. S. Ball and B. Farouk, Bifurcation phenomena in Taylor–Couette flow with buoyancy effects, *J. Fluid Mech.* (1989), in press.
18. K. S. Ball and B. Farouk, On the development of Taylor vortices in a vertical annulus with a heated rotating inner cylinder, *Int. J. Numer. Meth. Fluids* **7,** 857–867 (1987).

CARACTERISTIQUES DU TRANSFERT THERMIQUE POUR UN ESPACE ANNULAIRE ENTRE CYLINDRES COAXIAUX AVEC UN CYLINDRE TOURNANT

Résumé—Les caractéristiques du transfert thermique de deux cylindres coaxiaux, l'un des deux étant tournant, ont été étudiées expérimentalement dans le domaine des nombres de Taylor $(Ta)_m$ allant de 10^3 à 2×10^7, avec des nombres de Reynolds axiaux Re entre 50 et 1000. Les mesures de transfert massique de naphtaline sont effectuées pour obtenir les coefficients de transfert thermique. Quatre configurations de systèmes coaxiaux ont été choisies pour étudier les phénomènes fondamentaux qui ont lieu dans les espaces annulaires. Les surfaces des cylindres constituant l'espace annulaire sont toutes deux lisses ou l'une lisse et l'autre axialement rainurée. Des mesures de chute de pression ont été effectuées sur quelques configurations. Les résultats obtenus suggèrent qu'il y a un mérite potentiel d'autres recherches dans le cas où l'on souhaite des densités de flux thermique importantes.

WÄRMEÜBERGANG IM RINGRAUM ZWISCHEN EINEM RUHENDEN UND EINEM KOAXIAL ROTIERENDEN ZYLINDER

Zusammenfassung—Der Wärmeübergang im Ringraum zwischen einem ruhenden und einem rotierenden koaxialen Zylinder wurde experimentell bei Taylor-Zahlen $(Ta)_m$ von 10^3 bis 2×10^7 und axialen Reynolds-Zahlen Re von 50 bis 1000 untersucht. Der Stoffübergang von Naphthalin wurde gemessen, um die Wärmeübergangskoeffizienten zu bestimmen. Es wurden 4 Konfigurationen des koaxialen Systems ausgewählt, um grandsätzliche Phänomene zu untersuchen, die im Ringspalt auftreten. Die Oberfläche der Zylinder, die den Ringspalt bilden, waren entweder beide glatt, oder eine war glatt und eine mit axialen Nuten versehen. An einigen Anordnungen wurde der Druckabfall gemessen. Die bisherigen Ergebnisse lassen es nützlich erscheinen, die Untersuchungen in Gebieten hoher Wärmeübertragungsdichte fortzusetzen.

ХАРАКТЕРИСТИКИ ТЕПЛОПЕРЕНОСА В КОЛЬЦЕВОМ ЗАЗОРЕ МЕЖДУ ДВУМЯ СООСНЫМИ ЦИЛИНДРАМИ, ОДИН ИЗ КОТОРЫХ ВРАЩАЕТСЯ

Аннотация—Экспериментально исследуются характеристики теплопереноса для двух соосных цилиндров, один из которых вращается, причем значения чисел Тэйлора $(Ta)_m$ изменяются от 10^3 до 2×10^7, а аксиальные числа Рейнольдса изменяются от 50 до 1000. Коэффициент теплопроводности определяется на основе измерений массопереноса для нафталина. Для выяснения основных закономерностей теплопереноса в кольцевых каналах исследовано четыре варианта. Поверхности цилиндров, образующих кольцевые каналы, были гладкими, или одна из поверхностей была гладкой, а другая—рифленой в осевом направлении. Для некоторых конфигураций сначала измерялись перепады давления. Из полученных результатов следует, что целесообразно проведение дальнейших исследований данной проблемы для случая больших плотностей тепловых потоков.